Motion behavior of a charged droplet impacting on hydrophilic and hydrophobic leaf surfaces

Wei Hu,[1,2] Zhouming Gao,[1,2] Jian Chen,[1,2] Xiaoya Dong,[1,2] Baijing Qiu[1,2]

[1]School of Agricultural Engineering, Jiangsu University, Zhenjiang, Jiangsu; [2]Key Laboratory of Plant Protection Equipment, Ministry of Agriculture and Rural Affairs, Jiangsu University, Zhenjiang, China

Abstract

The impact behavior of charged droplets on leaf surfaces with varying degrees of hydrophobicity was experimentally investigated. A high-speed camera was employed to quantitatively capture the impact morphology and motion dynamics of the droplets under different conditions. The study primarily focused on analyzing the effects of three key parameters: static contact angle θ, applied voltage U, and droplet Weber number (We) on the droplet impact dynamics. The results revealed that droplets impacting hydrophobic surfaces exhibited smaller spreading diameters and higher retraction heights compared to those on hydrophilic surfaces. Furthermore, the maximum spreading ratio β_{max} of charged droplets on the leaf surface was reduced by approximately 10.8%, and the maximum recoiling height ratio H^*_{max} decreased by about 28% when compared to the behavior of neutral droplets. Additionally, the impact behavior of droplets on leaves under different We conditions was discussed. With the increase of droplet We from 59 to 175, droplet β_{max} increased by 34.9% and droplet H^*_{max} decreased by 24.1%.

Correspondence: Xiaoya Dong, School of Agricultural Engineering, Jiangsu University, Zhenjiang 212013, Jiangsu, China.
E-mail: dongxiaoya@ujs.edu.cn
Baijing Qiu, School of Agricultural Engineering, Jiangsu University, Zhenjiang 212013, Jiangsu, China. E-mail: qbj@ujs.edu.cn

Key words: charged droplet; droplets impact surface; plant leaves; impact dynamics; electrostatic spraying.:

Contributions: WH, BQ, conceptualization, methodology; WH, JC, software, formal analysis; WH, JC, ZG, investigation; WH, original manuscript drafting; BQ, manuscript review and editing, project administration, funding acquisition; XD, BQ, visualization, supervision. All authors have read and agreed to the published version of the manuscript.

Funding: This work was made possible by the National Natural Science Foundation of China (No. 31971790) and the Priority Academic Program Development of Jiangsu Higher Education Institutions (No. PAPD2023-87).

Received: 17 February 2025.
Accepted: 1 September 2025.

Journal of Agricultural Engineering 2025; LVI:1736
doi:10.4081/jae.2025.1736

Introduction

The impact behavior of liquid droplets on solid surfaces is a common phenomenon in nature (Gilet and Bourouiba, 2015; Roth-Nebelsick *et al.,* 2022). This phenomenon has broad applications across agriculture and industry, including crop protection spraying (Appah e*t al*., 2020, Gong *et al*., 2024), farm sterilization (White *et al*., 2018), surface coating (Wang *et al*., 2023), and power transmission (Deng *et al*., 2023). The dynamic behavior of droplets upon impact is influenced by various factors, such as surface properties, droplet velocity, and, notably, the droplet's charge, which can significantly alter the spreading, bouncing, or splashing characteristics. Understanding the complex interactions among these parameters is crucial for the precise control of droplet motion in various applications.

In agriculture, spraying is one of the most common methods for delivering pesticides and nutrients to plants. Specifically, the study of charged droplet dynamics has garnered attention due to its potential advantages in controlling deposition, improving surface wetting, and enhancing adhesion properties (Law, 2001). Appah *et al*. (2019) investigated the effects of parameters such as applied voltage, liquid flow pressure, and spraying height for pesticide application by induction charging. Wu *et al*. (2021) investigated the motion behavior of the strawberry leaves in an air-assisted spraying field and analyzed droplets deposition on the leaf surfaces. Salcedo and colleagues (2020) conducted field trials comparing the distribution of droplet deposition under different operational parameters, including wind speed, application of electrostatic charge, and travel speed. Dai *et al*. (2022) fitted a relationship curve between droplet size and charge-to-mass ratio at various voltages using Rayleigh's charge limit theory. Knight and colleagues (2022) quantified the effects of applied voltage, water mass flow rate, water conductivity, and spray pattern on the charge-to-mass ratio, finding that optimized configurations improved both droplet charging and poultry particulate matter collection efficiencies. Gao *et al*. (2023) measured the weight of plant roots before and after spraying and discussed the relationship between key operating parameters of high-voltage electrostatic ultrasonic atomizing nozzles and the droplets adhesion effect. The above studies primarily focused on optimizing electrostatic spraying system parameters, measuring the droplet charge-to-mass

ratio, and collecting deposition data on plant surfaces, recent research is shifting toward the microscopic scale of leaf surfaces (Ma *et al*., 2023). In particular, the motion behavior of charged droplets upon impacting the leaf surface is gaining increasing attention. The interaction between charged droplets and leaf surfaces not only influences the morphological and dynamic behaviors of the droplets but also plays a crucial role in charge transfer and adhesion behaviors (Hu *et al*., 2024). Thus, understanding the motion and charge generation mechanisms of charged droplets during their impact with leaf surfaces is essential for optimizing electrostatic spray systems and improving spray efficiency.

Research on the impact of charged droplets on solid surfaces began in the late 20th century, and with the advancement of technology, relevant studies have progressively deepened. Yatsuzuka *et al*. (1994) observed that neutral deionized water droplets sliding on a polymer plate exhibited sliding electrification. The droplets were positively charged, while the opposite polarity negative charge was deposited on the polymer plate, and the sliding speed of the droplets tended to stabilize with increasing sliding distance. Ryu and Lee (2009) experimentally investigated the motion behavior of droplets impacting a dielectric surface under different charge states and proposed a predictive model for the maximum spreading ratio of a charged droplet impact. The deviation between the model's calculations and experimental measurements was found to be less than ± 5%. Xu *et al*. (2021) further investigated the effect of surface temperature on the droplet impact behavior on the basis of the previous maximum spreading ratio prediction model. Although many research results have been achieved in studying the dynamics of charged droplet impacts, most of the studies have focused on the droplet impact behavior on synthetic surfaces, which generally possess better roughness and material uniformity. These synthetic surfaces cannot fully replicate the conditions of droplet impacts on natural leaves. Especially when a charged droplet impacts on the surface of natural leaves, the effects of three key parameters static contact angle of the surface q, applied voltage U and droplet Weber number We remain not fully understood. The static contact angle, which serves as a measure of surface wettability, determines the spreading and retraction behavior of the droplet, influencing whether it adheres, slides, or bounces. The Weber number, a dimensionless parameter that describes the ratio of inertial to surface tension forces, characterizes the droplet's ability to overcome surface tension and spread upon impact. Finally, the charging of the droplet introduces electrostatic forces that enhance the interaction between the droplet and the leaf surface, potentially altering the spreading, oscillation, or breakup behavior.

Despite ongoing research, the study of charged droplet impact on leaf surfaces remains insufficiently explored. The aim of this study is to investigate the effects of parameters such as , U and We on the dynamics of the impact of a charged droplet on the leaf surfaces. By adjusting and varying these experimental parameters, we hope to gain insight into the motion behavior of droplets under different voltages and dynamic conditions. The results of this study are important for improving the deposition of charged droplets on leaf surfaces in areas such as precision pesticide spraying, electrostatic inkjet printing, and electrostatic paint spraying technology.

Materials and Methods

Test materials

The seedlings of *Capsicum frutescens* L. (*C. frutescens*) were purchased online from a plant nursery (Shouhe, Shouguang City, Shandong Province, China). The seedlings were transplanted into 4L plastic pots and placed in greenhouses at the College of Agricultural Engineering, Jiangsu University (11°30'47'' E, 32°12'11'' N). The greenhouse conditions were monitored during the first 10 days of the experiment, with the average temperature ranging from 28°C to 38°C and relative humidity between 57 and 72%. The plants were watered once daily. *Epipremnum aureum* (*E. aureum*) were cultivated in the laboratory of the College of Agricultural Engineering, Jiangsu University, under controlled conditions with a temperature range of 24-32°C, relative humidity of 50-70%, and watering every two days. To minimize the impact of sharp temperature and humidity fluctuations on the physical state of the leaves and their dry matter content, the plants were acclimatized in the test environment for more than 48 hours before the experiment. This ensured that the leaves were well-adapted to the test conditions, reducing leaf deformation caused by environmental changes, and provided adequate water to maintain the health of the leaves. *Nelumbo nucifera* (*N. nucifera*) leaves and *Thysanolaena latifolia* (*T. latifolia*) leaves were collected in July 2024 from the university's campus landscape. Healthy leaves with intact surfaces, free from pests and diseases, were selected for experimental measurements. All tests were conducted within two hours of leaf collection to ensure leaf condition remained optimal.

Experimental setup

A syringe pump was connected to a polyethylene (PE) pipette, which was equipped with a filter. The PE tube was linked to a capillary with an inner diameter of 0.1 mm. The capillary was electrically grounded via a wire. The lower end of the capillary was positioned 10 mm above the center of a metal ring located directly below it. A 0-30 kV DC power supply (TCM6000i; Teslaman, Dalian, Liaoning, China) was connected to the metal ring to inductively charge the droplet. The charged droplet was then released and fell freely onto the surface of the fixed leaves placed below. The leaves used in the experiments were manually cut into rectangular sections of 30 mm × 20 mm in size. These sections were flatly adhered to a glass slide using double-sided adhesive tape, which was placed on an insulating surface for the test, as opposed to the usual grounding situation. The droplet impact velocity was controlled by adjusting the distance between the capillary and the leaf surface, which was varied at 10, 20, and 30 cm. A high-speed camera (i-Speed TR; Olympus Corp., Shinjuku, Tokyo, Japan) was positioned to capture the cross-sectional view of the droplet impact on the leaf surface. The light source was positioned directly in front of the camera lens, with the droplet impact area placed in between the camera and light source. This backlighting configuration allowed for optimal visualization of the droplet's impact morphology. The high-speed camera was connected to a PC for real-time image storage and analysis. To eliminate the influence of any residual charge on the leaf surface, which could affect the droplet's spreading behavior, a metal cylinder was rolled over the leaf surface before each droplet impact (Ryu and Lee, 2009). This procedure ensured that the leaf surface was charge-free prior to each test. Experimental setup was shown in Figure 1.

As reported by Mao *et al*. (1997), the static contact angle of a droplet on the surface is a critical parameter influencing the behavior of droplet impact motion. In addition, the charged state of the droplet and its impact velocity are also important factors. Therefore, the static contact angle, droplet size, and velocity were measured using an optical contact angle meter (OCA 25; Dataphysics, Filderstadt, Germany) and a high-speed camera prior to the commencement of the experiment.

Measurement of leaves samples

Leaf contact angle determination. Fresh healthy plant leaves were extracted, and considering that the contact angle of the droplets would be affected by the leaf veins (Xu *et al*., 2010), the primary and secondary leaf vein locations were avoided, and a flat portion of the leaf surface was intercepted at 20 mm × 20 mm, and the backside of the intercepted leaf was glued to the slide (length 76 mm, width 25 mm, height 1 mm) with double-sided adhesive, to obtain a spreading plant leaf surface (Lin *et al*., 2016). The static contact angle of the adaxial surface of the samples (droplet volume of 2 μL) was determined using an optical contact angle meter at room temperature. Leaves contact angle measurement was shown in Figure 2.

Measurement of droplet velocity and diameter

Measurements of droplet velocity and diameter were conducted using a high-speed camera (i-Speed TR, Olympus Corporation), a macro lens (AT-X Pro D 100 mm F2.8 macro lens; Kenko Tokina, Germany), and associated accessories. The camera parameters were set to a frame rate of 3000 FPS and a resolution of 1280 × 1024 pixels, based on the balance between the device's storage capacity (32 GB), image quality, and recording duration. Velocity and diameter measurements were performed in two stages. First, droplet velocities were measured for three release heights (10, 20, and 30 cm) to analyze the effect of different droplet velocities on the kinematic behavior of droplets impacting the surface of the leaves. Prior to the start of the experiment, the camera was calibrated using a standard ceramic calibration sphere (true roundness of 0.001 mm, repeatability of 0.0005-0.001 mm). High-speed images were processed automatically using MATLAB (vers. 2022b, The MathWorks Company, MA, USA).The image frame in which the lower end of the droplet first contacted the leaf surface was identified and designated as F_1.The image sequence was then played backward to locate the two preceding frames, which were labeled F_0 and F_{-1}. The time interval between consecutive frames Δt was determined from the recording frame rate $\Delta t = (F_0\text{-}F_{-1})$ / frame rate. The vertical distance of droplet centers between two frames S were measured, the time interval between the two selected images depended on camera frame rate F, allowing for terminal velocity v calculations for slower droplets using the equation:

$$\Delta t = \frac{F_0 - F_{-1}}{F} \quad \text{(Eq. 1)}$$

$$v = \frac{S}{\Delta t} \quad \text{(Eq. 2)}$$

where: Δt represents the time between two frames (s), F_0 represents the frame number in the first image, F_{-1} represents the frame number in the second image, F represents the frame rate selected by the camera (3000 (frames) /s), v represents the average speed (m/s) between two frames (due to the low speed droplet and small distance, it is assumed to be the instantaneous speed of the droplet hitting the surface of leaves), and S represents the vertical distance of droplet centers between two frames (mm). Since the freely released droplets from the capillary undergo a process of stretching and then breaking, it is necessary to observe that the droplet shape is approximated as a corresponding circle before measuring the droplet size. Assuming that the droplet is spherical, the equivalent droplet diameter D_0 can be expressed as (Ryu and Lee, 2009):

$$D_0 = \left(D_v {D_h}^2\right)^{\frac{1}{3}} \quad \text{(Eq. 3)}$$

where D_v and D_h are the vertical and horizontal diameters (mm) of the droplet, respectively. In this study, the equivalent diameter D_0 is considered as the initial diameter (mm) of the droplet. The procedure for velocity and size measurement of droplets was conducted according to the setup illustrated in Figure 3.

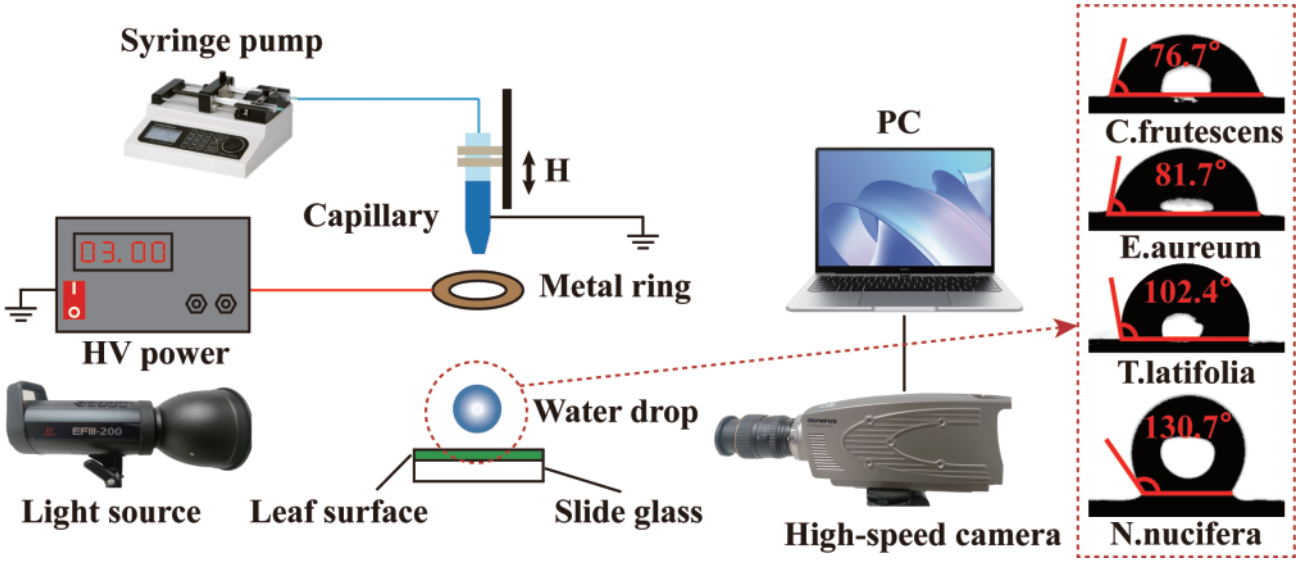

Figure 1. Experimental setup.

Results and Discussion

Neutral droplets impact hydrophilic/hydrophobic leaves

Static contact angle is an important parameter to study the motion behavior of droplets impacting the surface of plant leaves. The mean values of static contact angle measurements (θ = 76.7°, 81.7°, 102.4°and 130.7°) were obtained for four types of leaves, namely, *C. frutescens*, *E. aureum*, *T. latifolia* and *N. nucifera*, where the static contact angle of *C. frutescens* and *E. aureum* surfaces is less than 90° for hydrophilic surfaces, and on the contrary, *T. latifolia* and *N. nucifera* surfaces are hydrophobic surfaces.

Figure 4 presents a photograph of a neutral droplet impacting the surface of leaves with varying wettability at a velocity of 1.31 m/s (We = 59). The droplet impact process can be divided into three distinct stages: the spreading stage, the recoiling stage, and the oscillating stage. As shown in Figure 4a, upon initial contact with the surface of the *C. frutescens* leaf, the droplet begins to spread. After approximately 5 ms, the spreading diameter reaches its maximum value D_{max}, after which the droplet starts to recoil under the influence of surface tension, aiming to minimize the specific surface area. During the recoil phase, the spreading diameter decreases while the recoil height increases. The maximum recoil height H_{max} is achieved at around 19.3 ms, after which the droplet oscillates periodically due to the continuous exchange between kinetic and surface energy until it stabilizes on the subface with a fixed contact angle.

Figure 4 b,c shows similar droplet impact behavior on the surfaces of *E. aureum* and *T. latifolia* leaves, where the spreading, recoil, and oscillation phases mirror those observed on the *C. frutescens* surface. However, it is evident that with increasing hydrophobicity of the leaf surfaces (*E. aureum, T. latifolia*, and *N. nucifera*), the maximum spreading diameter decreases, while the maximum recoil height increases. The data further reveal that the

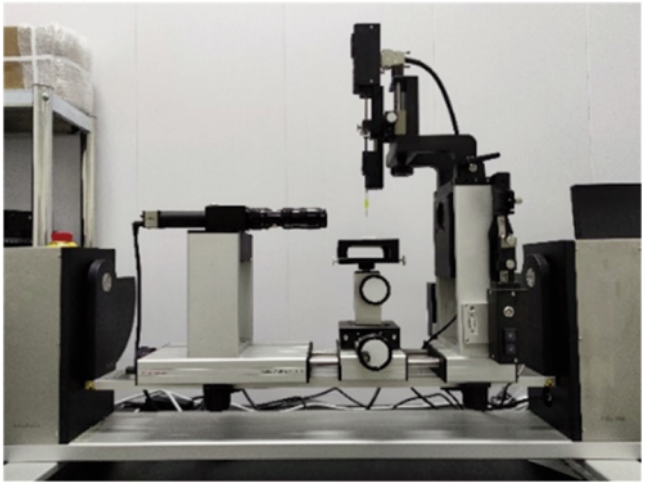

Figure 2. Leaf surfaces contact angle measurement.

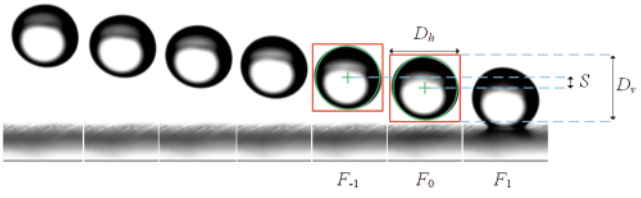

Figure 3. The procedure for velocity and size measurement of droplets.

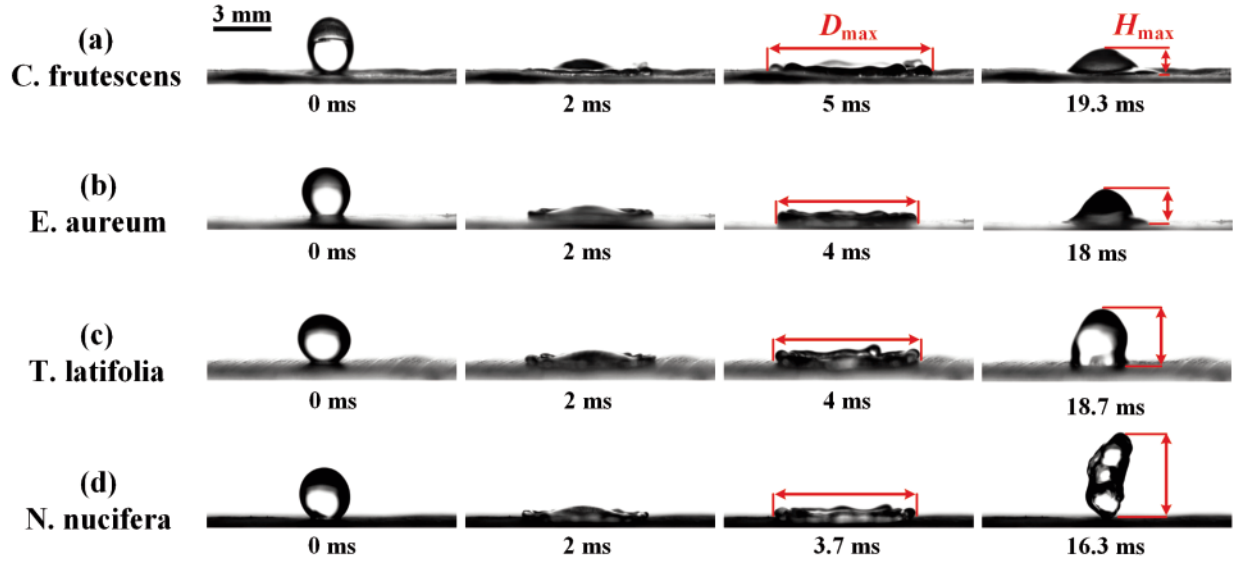

Figure 4. Snapshots of the neutral water droplet impact on (**a**) *C. frutescens*, (**b**) *E. aureum*, (**c**) *T. latifolia*, and (**d**) *N. nucifera*.

time to reach maximum spreading shifts from 5 ms on the *C. frutescens* leaf to 4 ms on the *E. aureum* leaf, 4 ms on the *T. latifolia* leaf, and 3.7 ms on the N. nucifera leaf, respectively. Conversely, the moments of maximum recoil occur earlier for more hydrophobic surfaces: 19.3 ms for the *C. frutescens* leaf, 18 ms for the *E. aureum* leaf, 18.7 ms for the *T. latifolia* leaf, and 16.3 ms for the *N. nucifera* leaf.

These differences in droplet impact behavior can be attributed to the wettability of the leaf surfaces, which directly influence the surface energy interactions. As described in previous studies (Mao *et al*., 1997), hydrophobic surfaces exhibit lower interfacial energy compared to hydrophilic surfaces, resulting in reduced viscous dissipation when droplets impact hydrophobic surfaces. In contrast, droplets impacting hydrophilic surfaces undergo greater viscous dissipation. For superhydrophobic surfaces, such as the *N. nucifera* leaf, only a small amount of energy is required to overcome this dissipation, and the energy conversion primarily occurs between the kinetic energy and surface energy of the droplet. This explains the observed droplet rebound phenomenon on superhydrophobic surfaces, as shown in Figure 4d for the *N. nucifera* leaf.

The extent of droplet spreading during impact is quantified using the spreading ratio *b*, which is a key parameter in the study of droplet dynamics. The spreading ratio reflects the degree of droplet spreading upon surface contact and is influenced by factors such as droplet size, velocity, surface tension, and surface wettability. In previous studies on droplet impact dynamics, the spreading ratio has been used to characterize the spreading behavior and to gain insights into the energy conversion mechanisms during the impact process. The *b* is defined as:

$$\beta = \frac{D_{max}}{D_0} \quad \text{(Eq. 4)}$$

where D_{max} and D_0 represent the maximum spreading diameter and the equivalent initial diameter of the droplet, respectively. Similarly, the recoiling height ratio H^* (where $H^* = H/D_0$) after droplet impact is expressed as the ratio of the droplet recoiling height H to the equivalent initial diameter D_0.

Figure 5 illustrates the variation of the spreading ratio of droplets over time on the surfaces of four different types of leaves. During the initial spreading phase—before the droplets reach their maximum spreading diameter—no significant differences are observed among the four curves. However, as the droplets approach their maximum spreading state, differences become evident. The droplets on the surface of the *N. nucifera* leaf are the first to achieve maximum spreading diameter, followed by those on the *T. latifolia* leaf, *C. frutescens* leaf, and *E. aureum* leaf in sequence. This observation suggests that the time required to reach the maximum spreading ratio for droplets impacting leaf surfaces at a single velocity is inversely related to the static contact angle of the leaf surface.

Interestingly, the maximum spreading ratio is highest on the *C. frutescens* surface, reaching approximately 2.74, while the *T. latifolia* leaf, *E. aureum* leaf, and *N. nucifera* leaf surfaces exhibit maximum spreading ratios of 2.69, 2.68, and 2.41, respectively. On hydrophilic leaf surfaces, such as those of *C. frutescens* and *E. aureum*, the droplets reach their maximum spreading state. Following this, the spreading ratio gradually decreases and eventually stabilizes at approximately 1.75 and 1.64, respectively. In contrast, droplets on hydrophobic surfaces, such as *N. nucifera* and *T. latifolia* leaves, retract rapidly after reaching the maximum spreading ratio. The spreading ratio drops to zero and the droplets rebound from the surface at approximately 20 ms and 25 ms, respectively. Figure 6 further demonstrates the variation of droplet recoiling height ratio over time on different leaf surfaces. During impact, the droplet height reaches a minimum when the droplet achieves its maximum spreading diameter, as the impact is dominated by kinetic energy. After this point, droplets on hydrophilic surfaces (e.g., *C. frutescens* and *E. aureum* leaves) begin to retract, leading to an increase in recoil height, which eventually stabilizes after a brief oscillation. The maximum recoil heights on *C. frutescens* and *E. aureum* leaves are approximately 1.53 mm and 1.40 mm, corresponding to recoil height ratios of 0.62 and 0.54, respectively. On hydrophobic surfaces (*e.g.*, *N. nucifera* and *T. latifolia* leaves), the maximum recoiling height ratios are significantly higher, reaching 2.05 and 1.63. Before the experiment, we hypothesized that the droplet would reach its maximum recoil height. At that stage, it marked the point where the droplet had recoiled upward to its maximum height, and the spreading diameter reached an extreme state—potentially nearing detachment from the leaf surface. Droplets possessed significant potential energy

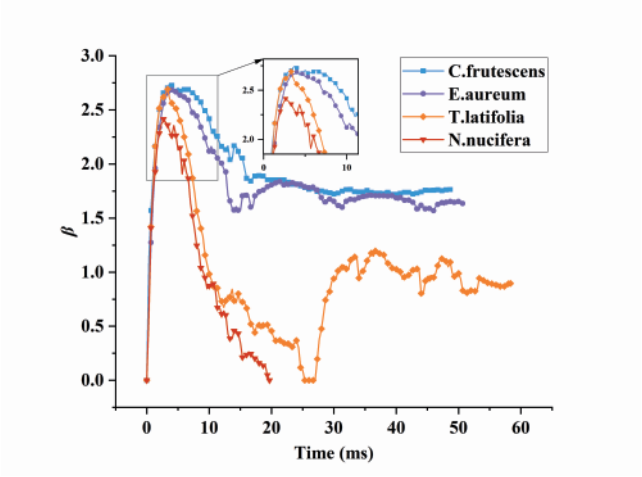

Figure 5. Variation of droplet spreading ratio with time on different leaf surfaces.

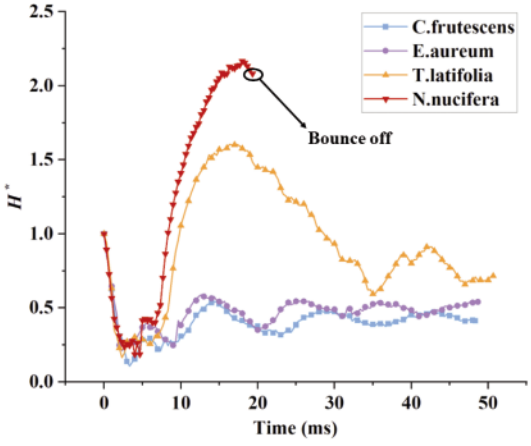

Figure 6. Variation of droplet recoiling height ratio with time on different leaf surfaces.

and surface energy at this phase, but no kinetic energy. However, the experimental results indicate that the droplet reaches its maximum recoil height before it fully bounces off the surface. For instance, the droplet reaches a maximum recoil height of 4.04 mm on the surface of the *T. latifolia* leaf at approximately 17.7 ms, while it only begins to leave the surface at around 25 ms, when the spreading diameter has nearly reduced to zero. This observation suggests that the spreading and recoil behaviors of droplets on the leaf surface should be analyzed separately, rather than relying solely on the spreading diameter for analysis.

Droplet impact behavior at different applied voltages

In addition to considering the wettability of the leaf surface, this study also investigates the influence of different voltages on the impact behavior of charged droplets impacting the surface of leaves. Figure 7 illustrates the impact behavior of charged droplets at varying voltages, with a velocity of approximately 1.31 m/s (We = 59) on the surface of *T. latifolia* leaves. As shown in Figure 7a, under the condition of 0 kV, which represents the impact of a neutral droplet, the maximum spreading diameter is about 7.57 mm, occurring at 4 ms. The droplet then reaches a maximum recoiling height of approximately 2.87 mm at around 18.7 ms after contacting the surface. In contrast, Figure 7b shows the motion of a charged droplet at 1 kV, where the spreading is noticeably less than that of the neutral droplet. The maximum spreading diameter is slightly reduced to 7.41 mm, and the maximum recoiling height decreases to 2.46 mm. Further increases in voltage to 2 kV and 3 kV, as depicted in Figure 7 c,d, lead to a more pronounced effect of the free charge on the droplet's motion behavior. At these voltages, the maximum spreading diameters decrease to 7.11 mm and 6.74 mm, respectively, and the spreading time is reduced from 4.3 ms to around 3.7 ms. With the increase in the applied external voltage, the maximum spreading diameter of the droplets was observed to decrease. This phenomenon can be attributed to the fact that both the leaf and the glass slide substrate are dielectric materials. Under the influence of the external electric field, the upper surface of the leaf becomes polarized, inducing a negative charge of the same polarity as that carried by the droplet. As a result, when the droplet approaches and impacts the leaf surface, electrostatic repulsion occurs between charges of identical sign, resisting the lateral spreading motion of the droplet. This repulsive effect reduces the kinetic energy available for spreading, thereby resulting in a smaller maximum spreading diameter. Similar observations have been reported in previous studies (Xu *et al*., 2024).This demonstrates the significant role that applied voltage plays in altering the dynamics of charged droplet impacts on leaf surfaces.

Figure 8 compares the variation of droplet spreading ratios at different voltages. Although the maximum and minimum spreading ratios differ, the changes in spreading diameter throughout the spreading process follow a similar trend across all four curves. After a charged droplet contacts the leaf surface, the droplet spreading ratio b increases rapidly from an initial value of 1 to a peak value, at which point the droplet height reaches its minimum. Following this, the droplet begins to retract, and the height increases as the spreading ratio gradually decreases, following a damped oscillatory pattern. Ultimately, the spreading ratio stabilizes at a fixed value due to the pinning effect of the surface (Theodorakis *et al*., 2021). It is also observed that the β_{max} of the charged droplets decreases as the voltage increases. Specifically, for neutral droplets under a velocity condition of We = 59, the maximum spreading ratio reaches approximately 2.83. However, for charged droplets at a positive voltage of 3 kV, the maximum spreading ratio decreases to around 2.53. As shown in Figure 9, the variation in the recoiling height ratio of charged droplets at different voltages is also clearly depicted. During the experimental measurement, the four curves exhibit periodic rises and falls, reflecting the energy conversion between the kinetic and surface energies of the droplets. The maximum recoiling height of the charged droplet significantly decreases with increasing applied voltage. This is primarily due to the enhanced electrostatic adhesion between droplets, which have relatively high surface charge densities, and the leaf surface (Li *et al*., 2023). The energy required to overcome this adhesion effect during droplet retraction is greater. Over time, energy is dissipated in the form of viscosity, and as a result, the retraction height decreases. Eventually, the droplet's kinetic energy is exhausted, and the droplet height stabilizes at a fixed value.

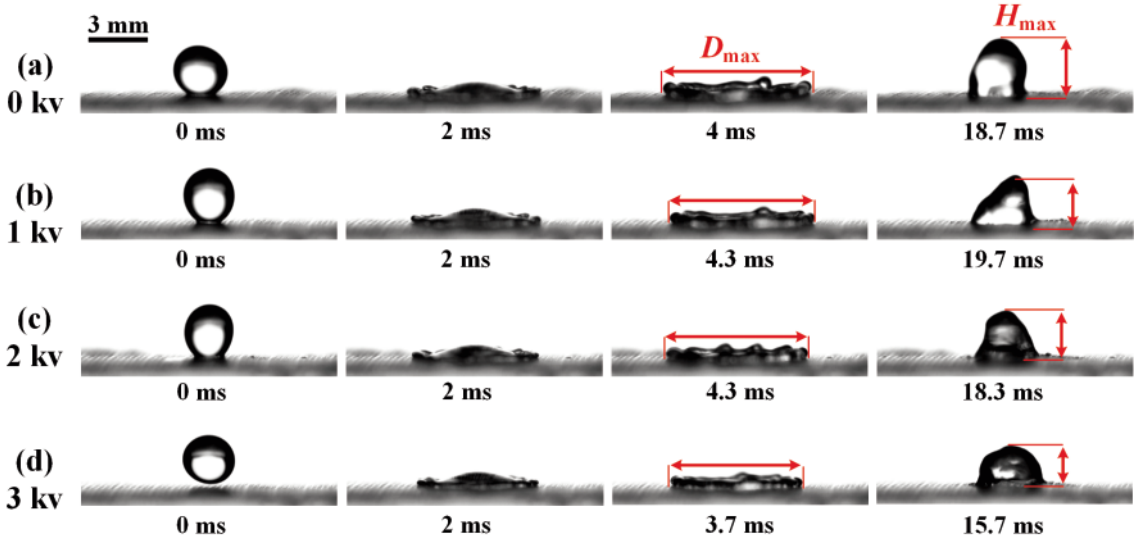

Figure 7. Droplet motion of a charged droplet impacting on the surface of a *T. latifolia* leaf at different applied voltages.

Effect of droplet We on impact behavior

The impact behavior of droplets of the same size impacting the surface of *T. latifolia* leaves at different Weber number (We = 59, 117, 175) was observed by adjusting the height of the capillary, releasing droplets from heights of 10, 20, and 30 cm. The curves presented in Figure 10 illustrate the variation in the spreading ratio of droplets with different We on the surface of the *T. latifolia* leaves over time.

Initially, the spreading ratio of the droplets increases rapidly upon contact with the surface of the leaves, reaching a maximum value near 4 ms. The maximum spreading ratios were 2.83 for We = 59 droplets, 3.74 for We = 117 droplets, and 4.36 for We = 175 droplets. The experimental data clearly show that the maximum spreading ratios of droplets of the same size increase with increasing We. This trend is due to the increased kinetic energy of the falling droplet, which causes them to spread outward upon impact. The spreading ratio continues to rise until the droplet reaches its maximum spreading diameter, after which the spreading ratio begins to decrease. This decrease marks the onset of the contraction behavior, where surface tension and viscosity begin to dominate. This decrease indicates that the droplet enters an oscillatory phase, undergoing a series of spreading and contraction cycles. In the post-impact phase, the balance between kinetic energy and surface tension leads to a repetitive cycle of spreading and recoil, with energy dissipated through viscous forces within the liquid and interactions with the surface (Kim and Chun, 2001). For the We = 175 droplets, the spreading ratio stabilized between 1.51 and 1.57 after approximately 33 ms of contact with the surface of the *T. latifolia* leaf, indicating that the droplet had reached a quasi-steady state. The extent of spreading and the subsequent retraction height also provide valuable information about the internal viscosity and surface tension of the droplets.

Figure 11 demonstrates the variation of the droplet recoiling height ratio with time, which exhibits a similar pattern to the spreading ratio curve. It shows that the droplet We significantly influences the recoiling height. After the droplet contact the sur-

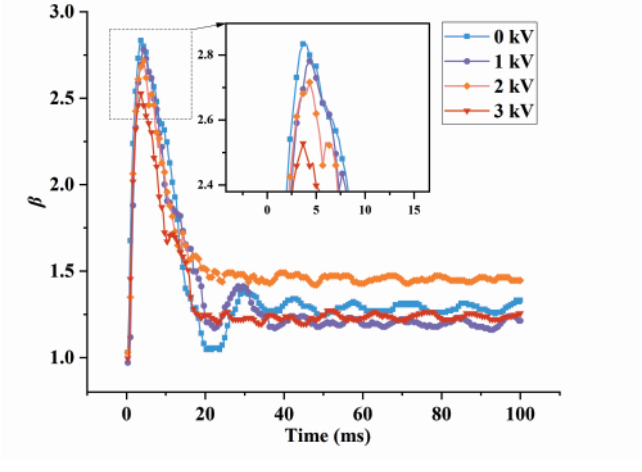

Figure 8. Spreading curves of a droplet impacting on the surface of *T. latifolia* leaf under different voltages.

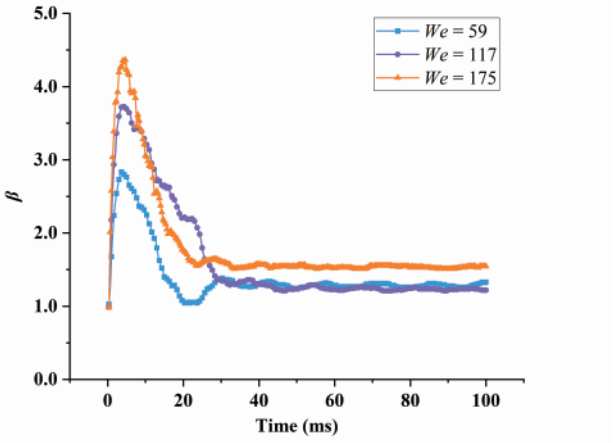

Figure 10. Spreading curves of a droplet impacting on the surface of *T. latifolia* leaf under different We.

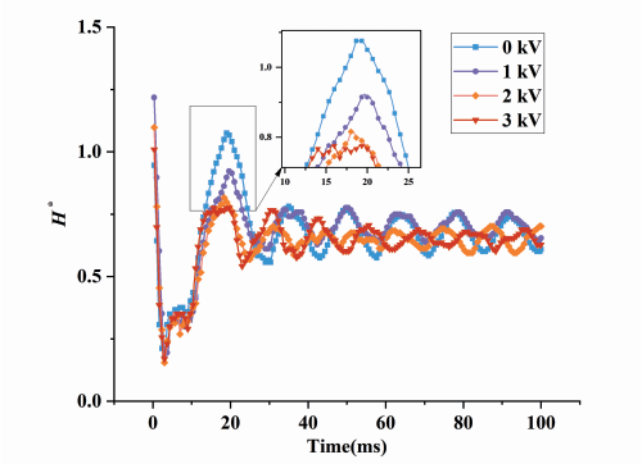

Figure 9. Recoiling curves of a droplet impacting on the surface of *T. latifolia* leaf under different voltages.

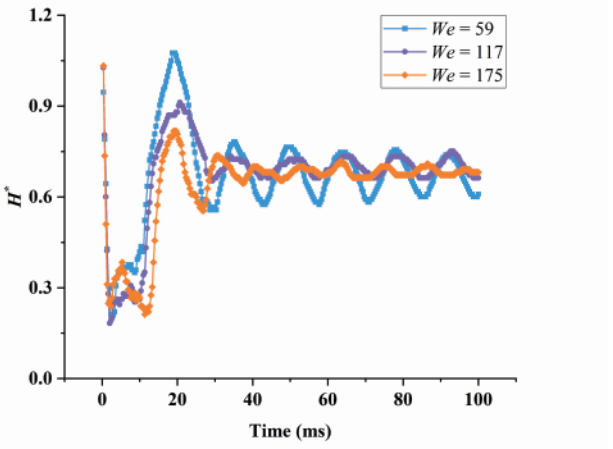

Figure 11. Recoiling curves of a droplet impacting on the surface of T. *latifolia* leaf under different We.

face of the *T. latifolia* leaves, the droplet height decreases rapidly until the maximum spreading diameter is reached. Subsequently, the droplets retract under the influence of surface tension and adhesion, causing the height to increase gradually. The maximum recoiling height is reached after about 20 ms of contact with the surface. The recoiling height ratio then decreases gradually, forming a periodic damped vibration. The maximum recoiling height ratios were 1.07 for We = 59, 0.90 for We = 117, and 0.82 for We = 175. These results reveal that the maximum recoiling height ratio decreases as the We increases when droplets of the same size impact the same leaf surface.

Overall, the experiment results provide a detailed view of the dynamic process of droplet spreading and recoiling, showing a distinct maximum followed by oscillations and eventual stabilization. This information is crucial for understanding the properties of liquids and surfaces and can be applied to various practical fields such as inkjet printing, spray cooling, and agricultural spraying.

Conclusions

In conclusion, the present study experimentally investigates the impact behavior of a charged droplet on leaf surfaces with varying wettability. By adjusting the capillary release height and the applied voltages, the kinematic behavior of droplets with We ranging from 59 to 175 and applied voltages between 0 and 4 kV was successfully captured. Four types of leaves with different wettability were used, consisting of two hydrophilic species (*C. frutescens* and *E. aureum*) and two hydrophobic species (*T. latifolia leaves* and *N. nucifera* leaves). The static contact angles for these leaves were 76.7°, 81.7°, 102.4°, and 130.7°, respectively.

The results show that the droplet impact behavior on hydrophilic leaves exhibited a larger spreading ratio and smaller recoil height compared to the behavior on hydrophobic leaves. Specifically, the data from the *T. latifolia* leaf surface indicate that the maximum spreading ratio β_{max} of charged droplets decreased by approximately 10.8%, and the maximum recoiling height ratio H^*_{max} was reduced by around 28.0% compared to neutral droplets.

This study highlights the significant role that free charge plays in the droplet spreading and recoiling processes. It also contributes to a deeper understanding of the kinematic behavior of charged droplets when impacting leaf surfaces, offering valuable insights for applications involving electrostatic spraying systems. Building on these findings, future research will extend beyond experimental measurements to incorporate theoretical analysis and numerical simulations. Specifically, subsequent work will investigate the impact behavior of charged droplets on substrates with different dielectric properties by comparing dielectric and conductive surfaces through experiments. Furthermore, a mathematical model for predicting the maximum spreading of charged droplets will be developed, along with criteria for determining their critical bouncing behavior.

References

Appah, S., Jia, W., Ou, M., Wang, P., Asante, E.A. 2020. Analysis of potential impaction and phytotoxicity of surfactant-plant surface interaction in pesticide application. Crop Prot. 127:104961.

Appah, S., Jia, W., Ou, M., Wang, P., Gong, C. 2019. Investigation of optimum applied voltage, liquid flow pressure, and spraying height for pesticide application by induction charging. Appl. Eng. Agr. 35:795-804.

Dai, S., Zhang, J., Jia, W., Ou, M., Zhou, H., Dong, X., H. et al. 2022. "Experimental study on the droplet size and charge-to-Mass ratio of an air-assisted electrostatic nozzle. Agriculture 12:889.

Deng, Q., Wang, H., Xie, Z., Zhou, X., Tian, Y., Zhang, Q., X. et al. 2023. Behaviors of the water droplet impacting on subcooled superhydrophobic surfaces in the electrostatic field. Chem. Eng. Sci. 266:118282.

Gao, J., Guo, Y., Tunio, M.H., Chen, X., Chen, Z. 2023. Design of a high-voltage electrostatic ultrasonic atomization nozzle and its droplet adhesion effects on aeroponically cultivated plant roots. Int. J. Agr. Biol. Eng. 162:30-37.

Gilet, T., Bourouiba, L. 2015. Fluid fragmentation shapes rain-induced foliar disease transmission. J. R. Soc. Interface 12:20141092.

Gong, C., Jia F., Kang, C. 2024. Deposition of water and emulsion hollow droplets on hydrophilic and hydrophobic surfaces. Agriculture 14:960.

Hu, W., Gao, Z., Dong, X., Chen, J., Qiu, B.J.A. 2024. Contact electrification of liquid droplets impacting living plant leaves. Agronomy (Basel) 14:573.

Kim, H.Y., Chun, J.H. 2001. The recoiling of liquid droplets upon collision with solid surfaces. Phys. Fluids 13:643-659.

Knight, R.M., Li, X., Hocter, J.S., Zhang, B., Zhao, L., Zhu, H. 2022. Optimization of induction charging of water droplets to develop an electrostatic spray scrubber intended for poultry particulate matter mitigation. T. ASABE 65:815-824.

Law, S.E. 2001. Agricultural electrostatic spray application: a review of significant research and development during the 20th century. J. Electrost. 51:25-42.

Li, X., Ratschow, A.D., Hardt, S., Butt, H.-J. 2023. Surface charge deposition by moving drops reduces contact angles. Phys. Rev. Lett. 131:228201.

Lin, H., Zhou, H., Xu, L., Zhu, H., Huang, H. 2016. Effect of surfactant concentration on the spreading properties of pesticide droplets on Eucalyptus leaves. Biosyst. Eng. 143:42-49.

Ma, J., Liu, K., Dong, X., Huang, X., Ahmad, F., Qiu, B. 2023. Force and motion behaviour of crop leaves during spraying. Biosyst. Eng. 235: 83-99.

Mao, T., Kuhn, D.C., Tran, H. 1997. Spread and rebound of liquid droplets upon impact on flat surfaces. AIChE J. 43:2169-2179.

Roth-Nebelsick, A., Konrad, W., Ebner, M., Miranda, T., Thielen, S., Nebelsick, J.H. 2022. When rain collides with plants-patterns and forces of drop impact and how leaves respond to them. J. Exp. Bot. 73:1155-1175.

Ryu, S.U., Lee, S.Y. 2009. Maximum spreading of electrically charged droplets impacting on dielectric substrates. Int. J. Multiph. Flow 35:1-7.

Salcedo, R., Llop, J., Campos, J., Costas, M., Gallart, M., Ortega, P., Gil, E. 2020. Evaluation of leaf deposit quality between electrostatic and conventional multi-row sprayers in a trellised vineyard. Crop Prot. 127:104964.

Theodorakis, P.E., Amirfazli, A., Hu, B., Che, Z. 2021. Droplet control based on pinning and substrate wettability. Langmuir 37:4248-4255.

Wang, T., Zhai, X., Huang, X., Li, Z., Zhang, X., Zou, X., Shi, J. 2023. Effect of different coating methods on coating quality and mango preservation. Food Packaging Shelf 39:101133.

White, D., Gurung, S., Zhao, D., Tabler, T., McDaniel, C., Styles, D., et al. 2018. Foam or spray application of agricultural chemicals to clean and disinfect layer cages. J. Appl. Poult. Res.

27:416-423.
Wu, S., Liu, J., Wang, J., Hao, D., Wang, R. 2021. The motion of strawberry leaves in an air-assisted spray field and its influence on droplet deposition. T. ASABE 64:83-93.
Xu, H., Wang, J., Wang, H., Li, B., Yu, K., Yao, J., et al. 2024. Numerical investigation of droplet impact and heat transfer on hot substrates under an electric field. Int. J. Heat Mass Transf. 229:125721.
Xu, H., Wang, J., Wang, Z., Yu, K., Xu, H., Wang, D., Zhang, W. 2021. Impact dynamics of a charged droplet onto different substrates. Phys. Fluids 33:102111.
Xu, L., Zhu, H., Ozkan, H.E., Thistle, H.W. 2010. Evaporation rate and development of wetted area of water droplets with and without surfactant at different locations on waxy leaf surfaces. Biosyst. Eng. 106:58-67.
Yatsuzuka, K., Mizuno, Y., Asano, K. 1994. Electrification phenomena of pure water droplets dripping and sliding on a polymer surface. J. Electrost. 32:157-171.